Alendronate-Decorated Nanoparticles as Bone-Targeted Alendronate Carriers for Potential Osteoporosis Treatment

Chunlan Jing[a], Bowen Li[a], Hui Tan[*b], Chang Zhang[a], Hongze Liang[a], Haining Na[c], Shenmao Chen[d], Chaozong Liu[d], Lingling Zhao[*abd].

[a]Faculty of Materials Science and Chemical Engineering, Ningbo University, Ningbo 315211, China.

[b]Department of Neurosurgery, The First Affiliated Hospital, Shenzhen University Health Science Center, Shenzhen, 518035, China.

[c]Ningbo Key Laboratory of Polymer Materials, Ningbo Institute of Materials Technology and Engineering, Chinese Academy of Sciences, Ningbo, Zhejiang 315201, China.

[d]Division of Surgery and Interventional Science, University College London, London HA7 4LP, U.K.

KEYWORDS: bone-targeted, osteoporosis, nanoparticles, alendronate, drug carrier

ABSTRACT: Osteoporosis is a skeletal disorder characterized by a low bone mass and density. Alendronate (Alen), a second-generation bisphosphonate drug, was indicated as first line regimen for the treatment of osteoporosis. However, the use of Alen has been limited due to its low bioavailability and gastrointestinal side effects. Herein,

Alen-decorated nanoparticles were prepared through ionic crosslinking between poly (lactic-co-glycolic acid) and β-cyclodextrin modified chitosan (PLGA-CS-CD) and Alen modified alginate (ALG-Alen) for Alen loading and bone-targeted delivery. Alen was selected as a therapeutic drug as well as a bone targeting ligand. The nanoparticles have negatively charged surfaces, and sustained release of Alen from the nanoparticles can be observed. Cytotoxicity detected by cell counting kit-8 (CCK-8) assay and lactate dehydrogenase (LDH) release test on MC3T3 cells showed that the nanoparticles had good cytocompatibility. Hemolysis test showed that the hemolysis ratios of nanoparticles were <5%, indicating that the nanoparticles had no significant hemolysis effect. Moreover, the Alen-decorated nanoparticles exhibited enhanced binding affinity to the hydroxyapatite (HAp) disks compared with that of nanoparticles without Alen modification. Thus, the Alen-decorated nanoparticles might be developed as promising bone-targeted carriers for the treatment of osteoporosis.

1. INTRODUCTION

Osteoporosis is the most frequent metabolic disease characterized by abnormal loss of bony tissue and a decrease in bone strength due to a microarchitectural deterioration of bone tissue, resulting in fragile porous bones and enhanced risk of fracture.[1-2] It became an actual and serious health problem since all osteoporotic fractures are associated with high morbidity, and some fractures affecting hip or vertebrae are even linked with high mortality.[3] Bisphosphonates are indicated as first-line treatment for osteoporosis due to their significant bone selectivity rather than other tissues. However, the bisphosphonates therapy of osteoporosis presents some

limitations, such as the low oral bioavailability (<1%) and the numerous side effects related to gastrointestinal tract.[4] For example, Alen is an active bisphosphonate molecule widely used in osteoporosis therapy, which presents an extremely low oral bioavailability, only 0.7%.[3] During the last decades, several studies have been presented to circumvent these shortcomings. Among them, encapsulation of Alen using particulate carrier systems holds great promise to enhance therapy efficiency and tolerance. Some approaches were also used to prepare particulate carrier systems, such as nanoprecipitation,[3] double emulsion-solvent evaporation,[5] ionic gelation[6] and so on.

Multi-functional nanoparticles play an importance role in drug delivery, and targeted nanocarriers are expected to improve the therapeutic efficacy of osteoporosis. Bisphosphonates including Alen, risedronate and etidronate are usually used as bone targeted ligands for drug delivery because they have high affinity with the main mineral component of bone (hydroxyapatite, HAp).[1,7] Ryu and coworkers[8] reported alendronate-conjugated nano-diamonds (Alen-NDs) as bone-targeted drug carriers for potential osteoporosis treatment. Alen-NDs exhibited high HAp affinity and could be specific uptaken by MC3T3-E1 cells. In addition, Alen-NDs enhanced ALP activity and displayed bone targeting ability in vivo due to the presence of Alen. Wang and coworkers[9] used alendronate to decorate mouse mesenchymal stem cells-derived extra-cellular vesicles (EVs) to generate Alen-EVs for osteoporosis therapy. Alen-EVs had high affinity with HAp in vitro and could protect against osteoporosis in ovariectomy (OVX)-induced osteoporotic rats with well tolerated and no side effects.

In this work, a novel nanocarrier for targeted alendronate delivery is prepared by ionic gelation between PLGA-CS-CD and ALG-Alen. Chitosan (CS) is the second most abundant nature polysaccharide with excellent biocompatibility, nontoxicity and

biodegradability.[10] Chitosan is regarded as a polymer with potential for bone targeting due to its positively charged.[11] It is reported to promote the cell adhesion and proliferation in bone forming due to its similar backbone of glycosaminoglycan, which is the main component of the extracellular matrix.[12] Poly (lactic-co-glycolic acid) (PLGA) has excellent biodegradability, biocompatibility and immune neutral properties. It is widely utilized in the fabrication of nano- and microparticle drug delivery systems and has been approved in the global market.[13-14] Recent studies indicated that CS-PLGA copolymer has the merits of both PLGA and CS and displayed better drug delivery promises.[15-16] On the other hand, cyclodextrin (CD) is a kind of α-1,4-linked cyclic oligosaccharides of D-glucopyranose with non-toxicity and biocompatibility. It is reported that CD could form inclusion complexes with bisphosphonate as bisphosphonate carriers due to its cage structure.[17] In this approach, β-cyclodextrin was conjugated to CS-PLGA copolymer for better encapsulation of alendronate. Alginate (ALG) is a natural anionic biopolysaccharide obtained from brown algae, and has been widely used for biomedical application due to its good water solubility, biocompatibility and low toxicity.[18] Previous reports showed that alginate-based drug carriers could improve the solubility of hydrophobic drugs[19] and inhibit the photodegradation of active compounds.[20] In this system, Alen was selected as a model drug as well as a bone targeting ligand. Herein, Alen-decorated polymeric nanoparticles were fabricated and their in vitro drug release behavior, cytotoxicity and affinity to HAp were evaluated.

2. Materials and methods

2.1 Materials

Chitosan (CS, M_W~100 kDa, 75% deacetylation) was kindly provided by Ningbo Haixin Biological Company, China. Poly (lactic-co-glycolic acid) (PLGA; lactide:glycolide 75:25; M_W~9500) was purchased from Dalian Meilun Biotechnology Co., Ltd. N-hydroxysuccinimide (NHS) was purchased from Quzhou Xinteng Chemical Co., Ltd. Alendronate ((4-amino-1-hydroxybutylidene) diphosphonate trihydrate, Alen) was purchased from Hewns (Tianjin) Technology Co., Ltd. Maleic anhydride (MA) was purchased from Shanghai Aladdin Bio-Chem Technology Co., Ltd. β-cyclodextrin (β-CD), nano-hydroxyapatite (HAp) and Fluorescein isothiocyanate isomer I (FITC) were purchased from Shanghai Macklin Biochemical Co., Ltd. Alginate (ALG) was purchased from Beijing Solarbio Science and Technology Co., Ltd. Rhodamine B (RB) was purchased from Shanghai Yuanye Bio-Technology Co., Ltd. 1-Ethyl-3-(3-dimethylaminopropyl) carbodiimide hydrochloride (EDC) and other solvents were purchased from Sinopharm Chemical Reagent Co., Ltd.

2.2 Synthesis of β-CD and PLGA modified CS (PLGA-CS-CD)

β-CD was grafted to CS using MA as a linker, and PLGA was grafted through amide reaction.[15] 0.2 g of CS (1.24 mmol) was dissolved in 20 mL of acetic acid solution (10 wt%). To this, 1 mL of MA solution (61.3 mg of MA dissolved in DMSO) was added dropwise. The mixture was stirred at 25 °C for 24 h, and then transferred to a dialysis tube (MWCO: 8~14 kDa). The mixture was dialyzed against distilled water for 3 days, and the water was changed every 4 h. The white cotton-like product CS-MA was harvested with a yield of ~85% by freezing dried.

222 mg of CS-MA was dissolved in 50 mL of acetic acid solution (10 wt%), and

179.7 mg of EDC (0.94 mmol) and 71.9 mg of NHS (0.63 mmol) was added. The mixture was stirred at 25 °C for 3 h. Then, 709.4 mg of β-CD dissolved in 5 mL of DMSO was added dropwise and stirred for another 24 h under room temperature. The residue was transferred to a dialysis tube (MWCO: 8~14 kDa) and dialyzed against distilled water for 3 days. The white cotton-like product CS-CD was harvested with a yield of ~85% by freezing dried.

210 mg of CS-CD was dissolved in acetic acid solution (10 wt%, 10 mL). 0.2 g of PLGA (0.02 mmol), 14.8 mg of EDC (0.08 mmol) and 6.1 mg of NHS (0.05 mmol) was dissolved in DMSO (35 mL). The mixture was stirred at 25 °C for 2 h followed by adding to the CS-CD solution. After 24 h, the residue was transferred to a dialysis tube (MWCD: 8~14 kDa) and dialyzed against distilled water for 3 days. The white cotton-like product PLGA-CS-CD was harvested with a yield of ~76% by freezing dried.

2.3 Synthesis of alendronate modified alginate (ALG-Alen)

ALG-Alen was synthesized according to a similar procedure previously reported.[21-22] In brief, 81.3 mg of Alen (0.25 mmol) was dissolved in 12.5 mL of 10% aqueous acetic acid solution. The mixture was freeze dried and resuspended with 6 mL of distilled water. 99 mg of ALG (0.5 mmol), 47.9 mg of EDC (0.25 mmol) and 19.2 mg of NHS (0.17 mmol) was dissolved in H_2O (8 mL). After being stirred at 25 °C for 2 h, the acidified Alen dispersion was added to the activated ALG and allowed the reaction to continue for 24 h. The product was purified by dialysis against water, and preserved at cold temperatures for further use (yield, ~57%).

2.4 Synthesis of FITC labelled alendronate (FITC-Alen)

FITC-Alen was synthesized according to a similar procedure previously reported.[8] Briefly, 312.1 mg of Alen (0.96 mmol) was dispersed in 200 mL of H_2O, and 60 mg of

FITC (0.15 mmol) was dissolved in 100 mL of mixture solvent (CH_3OH: H_2O, 3.5:1, v/v). The FITC solution was added dropwise to the Alen dispersion, and stirred under room temperature in dark for 24 h. The methanol was removed by rotary evaporation, and the residue was freeze dried. The product was washed by methanol 3 times to remove the excess FITC, collected by centrifugation, and dried by oven (yield, 73%).

2.5 Preparation of empty and alendronate loaded nanoparticles

The nanoparticles were prepared using a similar method as previously reported.[23] Different nanoparticles can be prepared by changing the feed ratio of PLGA-CS-CD and ALG-Alen. Alendronate was labelled with FITC for quantitative analysis by fluorescence. PLGA-CS-CD was dissolved in the mixture of 10% aqueous acetic acid solution and DMSO with a volume ratio of 1:1 at a concentration of 5 mg mL^{-1}. To this, 9 mg of FITC-Alen dissolved in 1 mL of distilled water was added dropwise, and the mixture was stirred at 25 ºC for 1 h. Then, different amount of ALG-Alen aqueous solution (5 mg mL^{-1}) was added to the PLGA-CS-CD/FITC-Alen solution, and stirred vigorously for another 1 h. The precipitate was collected by centrifugation, and then washed by H_2O three times. The residual FITC-Alen in the supernatant was measured by fluorescence spectrophotometer using the calibration curve obtained from FITC-Alen PBS solution. The drug loading content (DLC) and loading efficiency (LE) was calculated as follow:

$$\text{DLC}(\%)=\frac{\text{drug fed amount-drug in supernatant}}{\text{nanoparticles amount}}\times 100\%$$

$$\text{LE}(\%)=\frac{\text{drug fed amount-drug in supernatant}}{\text{drug fed amount}}\times 100\%$$

Empty nanoparticles without drug loading were prepared as described above by

adding equal distilled water instead of FITC-Alen solution.

For the HAp affinity test, RB was used to label the empty nanoparticles. In brief, 6 mg of RB (0.0125 mmol), 15.5mg of EDC (0.04 mmol) and 0.65 mg of DMAP (0.00267 mmol) was dissolved in 3 mL of H_2O, and the mixture was stirred for 30 min. 30 mg of ALG (0.15 mol) was dissolved in 7.5 mL of H_2O. Subsequently, the RB solution was added dropwise to the ALG solution under stirring at 37 °C. After stirring for another 24 h, the mixture was transferred to a dialysis tubing (MWCD: 8~14 kDa) and dialyzed for 3 days. The product was obtained by freeze dried (yield, 79%). All steps were done in dark. RB-ALG-Alen was synthesized using the same procedure as described above. The preparation process of nanoparticles was described above. As shown in Table 1, 8 different nanoparticles were prepared.

Table 1. Preparation parameters of different nanoparticle formulations

Sample	Volume of PLGA-CS-CD solution (mL)	Volume of ALG-Alen solution (mL)	Volume of FITC-Alen solution (mL)	Volume of RB-ALG-Alen solution (mL)	Volume of RB-ALG solution (mL)	Ratio of PLGA-CS-CD to ALG
$NP1_{Alen}$	4	2	1	—	—	2:1
$NP2_{Alen}$	3	3	1	—	—	1:1
$NP3_{Alen}$	2	4	1	—	—	1:2
$NP1_{Emp}$	4	2	0	—	—	2:1
$NP2_{Emp}$	3	3	0	—	—	1:1
$NP3_{Emp}$	2	4	0	—	—	1:2
$NP4_{RB}$	3	—	0	3	—	1:1
$NP5_{RB}$	3	—	0	—	3	1:1

2.6 Characterization

^{1}H NMR spectra was performed on Bruker AMX 400 MHz spectrometer (Bruker Swiss). Infrared spectroscopy analysis was detected at Nicolet 6700 Fourier infrared spectrometer (Thermo Nicolet. USA) from 4000 to 400 cm^{-1}. The morphology of nanoparticles was observed by Hitachi S-4300 (Nova NanoSEM 450，FEI. USA) at an operating voltage of 15 kV. The nanoparticle dispersion was dropped onto a tinfoil, air-dried and then glue on a sample table for observation. The Zeta potential and particle size was tested using a Malvern Zana ZS 90 Mastersizer (MAHlvern Panalytical. US). The samples were dispersed in H_2O at 0.1 mg mL^{-1}, and ultrasonic in YJ-5200D ultrasonic instrument (Ningbo Yongjie Instrument Co., LTD) for 3 min before test.

2.7 *In vitro* drug release

In vitro release behavior of alendronate from the nanoparticles was conducted through dialysis method using phosphate buffer solution to simulate the human physiological environment. Briefly, 3 mg of nanoparticles were dispersed in PBS (1 mL), respectively, and then transferred to a dialysis tube (MWCO: 8~14 kDa). The tubes were immersed into a brown vial containing 10 mL of PBS and incubated in a water bath at 37 ºC. At regular time intervals, 3 mL of release medium was withdrawn and replaced with 3 mL of fresh PBS. The amount of released alendronate was measured using fluorescence spectrophotometer. The excitation and emission wavelength were 495 and 520 nm, respectively. The release experiment was conducted in tow parallel experiments, and the results were expressed as the mean value with standard deviations.

2.8 Cytotoxicity test

The cytotoxicity of nanoparticles was measured using CCK-8 assay and LDH release test. Well-growing MC3T3 cells were seeded onto 96-well plates at a density of 8000 cells per well in 100 μL of culture medium. The cells were incubated in the incubator at 37 ºC for 24 h. Then the medium was removed and replaced with 100 μL of medium containing various amounts of nanoparticles. After 24 h incubation, the medium was discarded and the wells were rinsed gently with PBS three times. Then, the wells were refilled with 100 μL of medium containing 10 μL of CCK-8 solution. After incubation for another 2 h, the absorbance at 450 nm of each well was measured using a microplate reader. The cell viability was expressed as the average data of six duplications with standard deviations using the following equation: Cell viability (%) $= \frac{Ab_S}{Ab_{con}} \times 100$, where Ab_s is the absorbance of cells incubated with nanoparticles, and Ab_{con} is the absorbance of cells incubated with medium only.

For the LDH release test, MC3T3 cells were seeded onto 96-well plates at a density of 1×10^3 cells per well in 100 μL. After 24 h incubation, the medium was removed and replaced with sample solution at different concentration. Cells were incubated at 37 ºC for another 24 h. The LDH Cytotoxicity Assay Kit (C0016, Beyotime, China) was used to detect the cell viability following the manufacturer's instructions. The LDH release was expressed as the average mean of six duplications with standard deviations using the following equation: LDH release (%) $= \frac{Ab_S - Ab_{con}}{Ab_{max} - Ab_{con}} \times 100$, where Ab_s is the absorbance of the cells incubated with nanoparticles and treated with LDH assay, Ab_{con}

is the absorbance of cells incubated with culture medium only, and Ab_{max} is the absorbance of cells incubated with culture medium and treated with LDH assay.

2.9 Hemolytic test

Whole blood was collected from healthy goats and diluted in PBS at 4%. Red blood cells (RBCs) were separated by centrifugation at 1500 rpm for 5 min three times to remove the plasma supernatant. Then, the erythrocytes were re-suspended in PBS at a density of $2x10^8$ cells/mL. 200 μL of the as-prepared RBCs suspension was incubated with 200 μL of sample solution at different concentrations at 37 °C for 1 h. Meanwhile, sterile water and PBS were used as positive and negative control, respectively. Then, the mixture was centrifuged at 1500 rpm for 5 min and the supernatant was transferred to another 96-well plate. The absorbance at 540 nm was recorded using a microplate reader (Thermo MULTISKAN MK3). The hemolysis rate was calculated using the equation as follows: $\text{Hemolysis}\ (\%) = \frac{Ab_s - Ab_{nc}}{Ab_{pc} - Ab_{nc}} \times 100$, where Ab_s, Ab_{nc}, and Ab_{pc} are the absorbance of the sample, the negative control, and the positive control, respectively.

2.10 Affinity of nanoparticles to HAp disk

HAp disks with a diameter of 1 cm (100 mg/disk) prepared by compression moulding (FYD 40, Tianjin Sichuang Jingshi Technology Development Co., Ltd.) were used to evaluate the HAp affinity of nanoparticles. In brief, 5 mL dispersion of empty nanoparticles (1 mg mL^{-1} in normal saline, 5 mL) with or without Alen decoration was incubated with HAp disks in a brown vial for 0.5, 2 and 4 h in dark. The absorbance of

dispersion was analyzed using a UV/vis spectrophotometer at 553 nm. The binding ratio to HAp was defined as the reduction in the percentage of absorbance at 553 nm. The HAp disks were gently washed with water and then imaged using Image Station (Leica TCS SP5 II laser confocal microscope). Both nanoparticles were tested in triplicate.

3. RESULTS AND DISCUSSION

3.1 Synthesis and Characterization of PLGA-CS-CD

The synthesis procedure of PLGA-CS-CD was shown in Scheme 1A. β-CD was conjugated to the CS using MA as a linker, and PLGA was grafted through the reaction between the carboxylate group in PLGA and the amino group in CS. Figure 1 shows the FTIR spectra of PLGA-CS-CD, CS-MA, CS-CD, PLGA and CS. As for CS-MA, the absorption bands at 1637 and 1560 cm^{-1} were assigned to the amide I and II vibration bands of CS,[21-23] and the peak appeared at 1712 cm^{-1} was assigned to C=O stretching vibration of -COOH,[24] indicating the successful amidation of CS and MA. The FTIR spectrum of CS-CD showed the disappeared peak at 1712 cm^{-1} for carbonyl groups and the stretching vibration of C-OH and -COO- for β-CD with strong intensity at 1030 and 1155 cm^{-1},[25-26] suggesting that successful esterification has occurred between β-CD and CS-MA. As for PLGA-CS-CD, the peak at 1758 and 1190 cm^{-1} represented the C=O and C-O-C stretching of PLGA,[27] indicating the successful conjugation of PLGA to CS. Figure 2 represents the ^{1}H NMR spectra of CS-MA, CS-CD and PLGA-CS-CD. For CS-MA, the broad peaks between δ 3.24 and 3.43 were attributed to the protons on C2-C6 of CS unit,[28] and the peak at δ 5.97 was attributed to the proton of CH=CH on maleic

acid unit. Compared with CS-MA, the peaks between δ 3.24 and 3.43 increased in the ^{1}H NMR spectrum of CS-CD due to the overlap of the protons peak on C2-C6 of CS and CD units,[29] and the peak at δ 5.97 decreased, suggesting the successful conjugation of β-CD to CS. For PLGA-CS-CD, the peak at δ 1.40 indicated the presence of CH_3 on side group of PLA in PLGA, the peak at δ 3.69 is attributed to the hydrogen bond to C2 of CS ring.[15,30] All these results suggested the successful synthesis of PLGA-CS-CD.

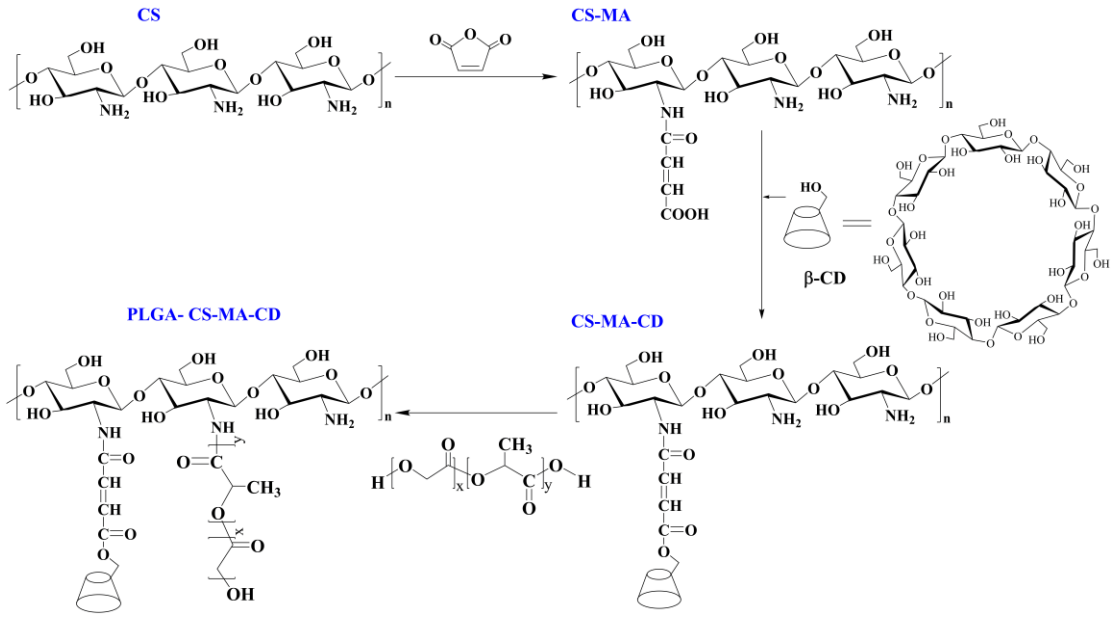

(A)

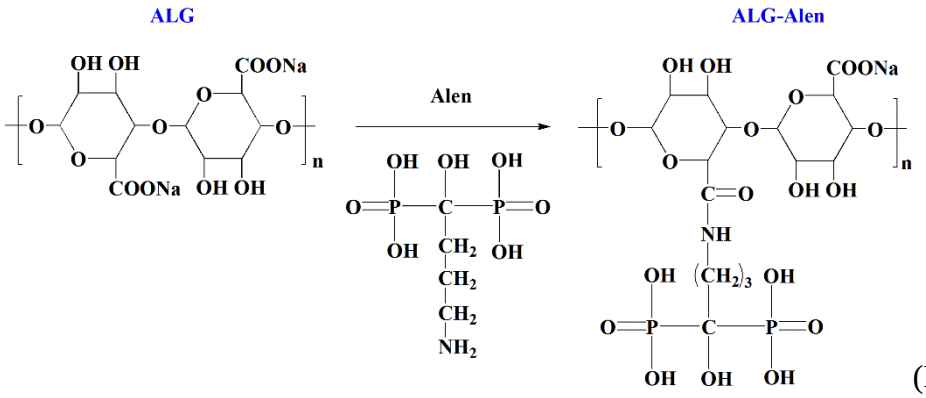

(B)

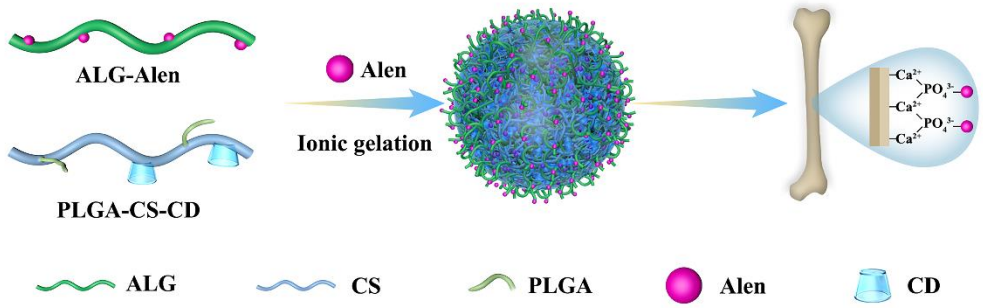

Scheme 1. Illustrative synthesis of PLGA-CS-CD (A), ALG-Alen (B), and Alen-decorated nanoparticles for bone-targeted delivery (C).

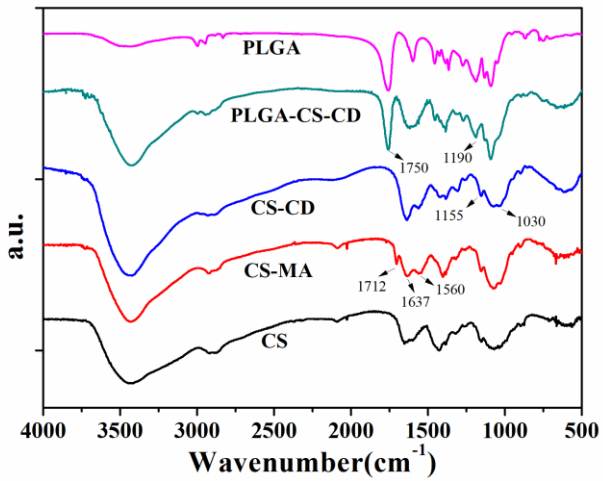

Figure 1. FTIR spectra of PLGA-CS-CD, CS-MA, CS-CD, PLGA and CS.

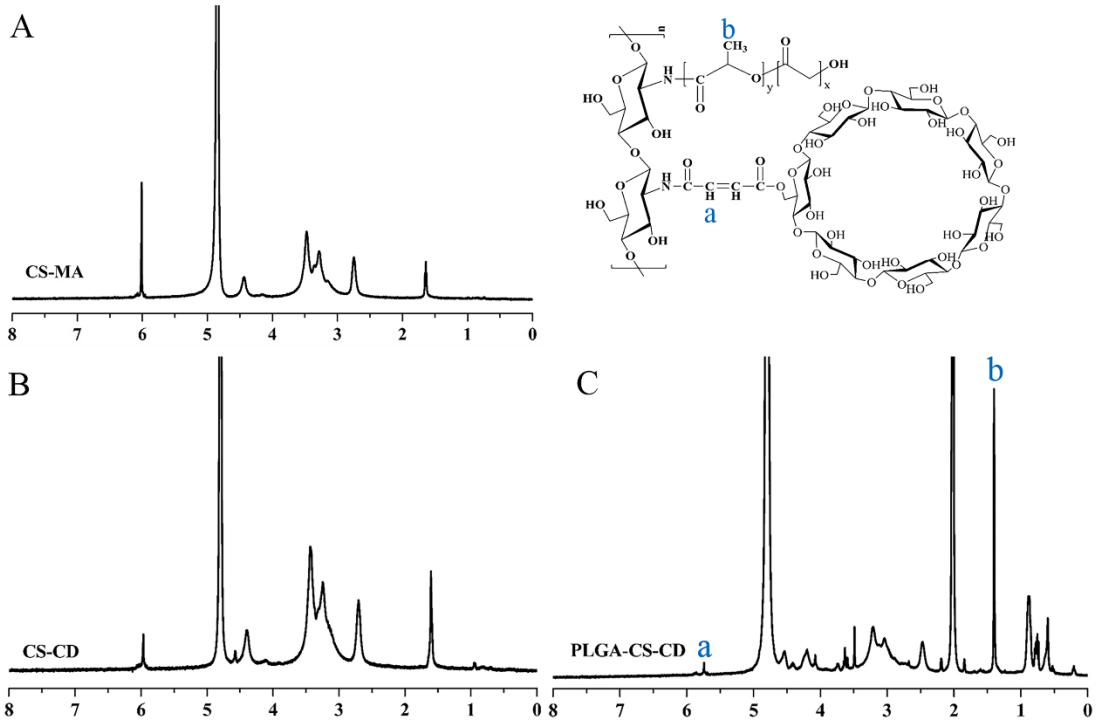

Figure 2. ^{1}H NMR spectra of CS-MA (A), CS-CD (B) and PLGA-CS-CD (C).

3.2 Synthesis and Characterization of ALG-Alen

ALG-Alen was synthesized through amidation between the amino group in alendronate and the carboxyl group in alginate, as shown in Scheme 1B. Figure 3 represents the FTIR spectra of ALG-Alen, ALG, and Alen starting materials. FTIR spectrum of ALG exhibited absorption bands at 3420 cm^{-1} for O-H stretching, peaks at 1028 cm^{-1} for C-O-C stretch, and at 1608 and 1416 cm^{-1} for COO- asymmetric and symmetric stretching.[21] As for Alen, the peaks at 1059, 1126, 1173, and 1238 cm^{-1} are assigned to the O=P-O stretches and H-O-P stretches in the structure of Alen, and the peak at 1654 cm^{-1} are attributed to the vibration of amine group. The specific peaks at 1614 and 1413 cm^{-1} for -COO- can be seen in the FTIR spectrum of ALG-Alen, including peaks at 1171, 1125 and 1029 cm^{-1} for PO_3 group,[31] which suggested the successful amidation between ALG and Alen. Figure 4 represents the ^{1}H NMR

spectrum of ALG-Alen. As shown, the broad peaks at δ 3.84-4.08 were attributed to the protons on C2-C6 of ALG unit. The peaks at δ 1.83 and 2.81 attributed to the protons on methylene groups of Alen,[21] indicating the successful synthesis of ALG-Alen.

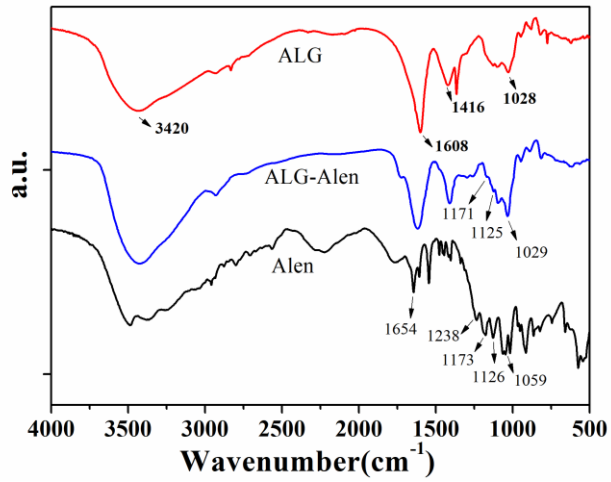

Figure 3. FTIR spectra of Alen, ALG and ALG-Alen.

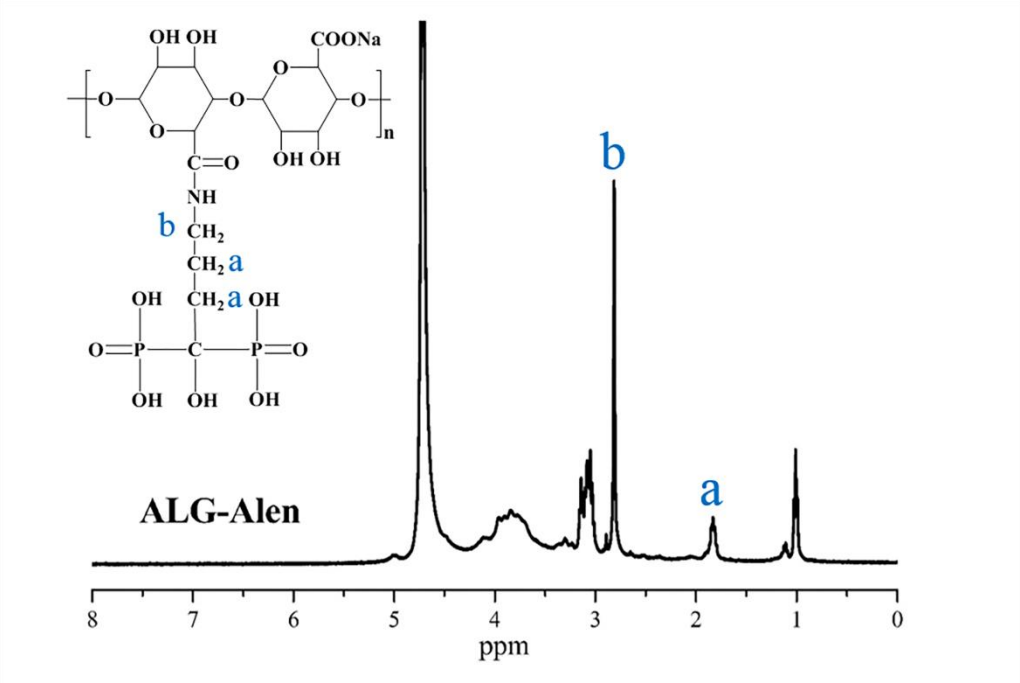

Figure 4. ^{1}H NMR spectrum of ALG-Alen.

3.3 Nanoparticles characterization

SEM images showed that nanoparticles prepared by different polymer ratio were in regular spherical shape with a diameter in the range of 200-400 nm (Figure 5A). Table 2 shows the hydrodymamic diameter and Zeta potential of the nanoparticles. The relative stability of the nanoparticles was confirmed by incubating the nanoparticles in distilled water for 48 h, and the particle sizes were measured using DLS at intervals. In Figure 5C, the sizes of nanoparticles at room temperature had a slight fluctuation within 48 h, possibly owing to the drug release and the swelling of nanoparticles during the incubation time. Zeta potential indicates that the surface of the nanoparticles was negatively charged, and the surface negative charge increased with the increase of ALG-Alen content (Figure 5D). For the RB labeled nanoparticles without alendronate ($NP4_{RB}$ and $NP5_{RB}$), the surface negative charge was lower than that of $NP1_{Alen}$, which was obtained by the same polymer ratio. This may be caused by the RB modification of alginate, as RB is positive charged. What's more, the negative charged surface of the nanoparticle formulations indicated the distribution of the bone targeting ligand (alendronate) on the surface of nanoparticles, because alendronate is modified on the negatively charged alginate, which is of great importance to the bone targeting ability of the nanoparticles.

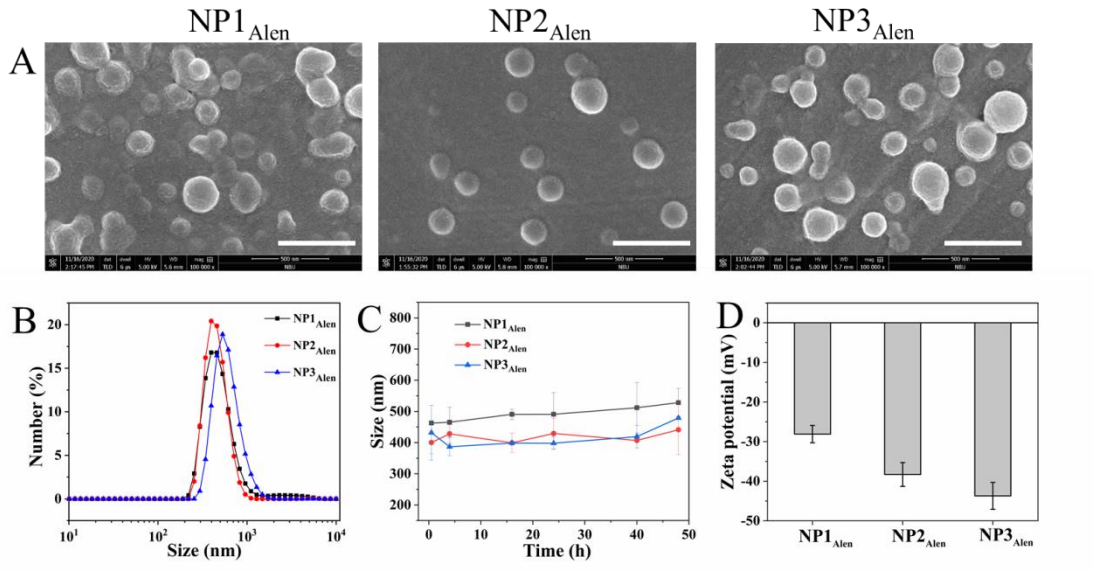

Figure 5. SEM images (A), particle size distribution (B), variation of particle size with time (C) and Zeta potential (D) of $NP1_{Alen}$, $NP2_{Alen}$ and $NP3_{Alen}$. Scale bar 500 nm.

Table 2. Characterization of nanoparticle formulations

Sample	Hydrodynamic diameter (nm)[a]	Zeta potential (mV)	LE (%)	DLC (%)
$NP1_{Alen}$	463±6	-28.1±2.2	70.7±5.6	54.6±8.8
$NP2_{Alen}$	400±36	-38.3±3.0	68.6±2.9	45.4±2.1
$NP3_{Alen}$	432±88	-43.7±3.4	53.3±1.3	42.9±7.3
$NP4_{RB}$	482±12	-22.4±1.8	—	—
$NP5_{RB}$	464±30	-24.8±1.9	—	—

[a] Measured by DLS.

3.4 In vitro drug release

As shown in Figure 6, nanoparticles with different formulations provide sustained release of Alen in PBS (pH 7.4) and the release profile was different depending on

PLGA-CS-CD/ALG-Alen ratio. In fact, the rate of Alen release increased with the increase of ALG-Alen ratio in the nanoparticles. In the first 30 min, Alen released from $NP1_{Alen}$ (PLGA-CS-CD/ALG-Alen ratio is 2:1) is 12.6%. At the same period, 19.4 and 20.7% of encapsulated Alen was release form $NP2_{Alen}$ (PLGA-CS-CD/ALG-Alen ratio is 1:1) and $NP3_{Alen}$ (PLGA-CS-CD/ALG-Alen ratio is 1:2), respectively. Kinetic equilibrium was reached in 22 h for $NP1_{Alen}$ and $NP2_{Alen}$. By this time, 73.2 and 79.3% of encapsulated Alen was released, and then slightly increased to 75.3 and 82.0% at the end of the study (72 h) for $NP1_{Alen}$ and $NP2_{Alen}$, respectively. While for $NP3_{Alen}$, equilibrium was reached in 11 h, and 93.0% of encapsulated Alen was released. This may be caused by the different content of PLGA-CS-CD in the nanoparticles. It is reported that cyclodextrin could form cyclodextrins-alendronate complexes,[17] and the inclusion complexes could slow down the release of Alen from the nanoparticles. However, the release kinetics of three different formulations presented a similar situation, with a burst release in the initial stage and a prolonged release in the later stage. The initial release phase might be due to the release of Alen absorbed on the nanoparticles surface.[6] According to reported studies, the Ritger-Peppas equation ($\frac{M_t}{M_\infty} = kt^n$) could be used to describe the drug release kinetics, where M_t / M_∞ is the cumulative release of drug at time *t*, and *n* is the diffusion-dependent component.[3] The calculated *n* values for Alen released from the nanoparticles based on Figure 6 in the first 22 h were 0.24, 0.15 and 0.42 for $NP1_{Alen}$, $NP2_{Alen}$ and $NP3_{Alen}$, respectively, indicating the drug release follows Fickian diffusion mechanism.

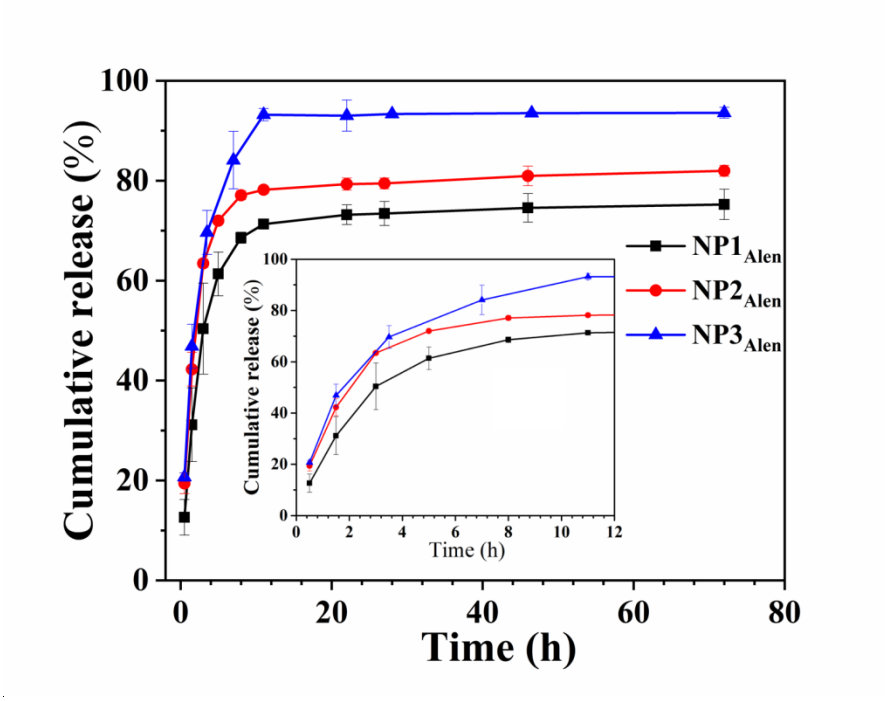

Figure 6. In vitro release of alendronate from different nanoparticles in PBS (pH 7.4) at 37 °C. The inset is the release profile at the first 11 h.

3.5 In vitro cell cytotoxicity

The cytotoxicity of the nanoparticles was evaluated in vitro by CCK-8 assay and LDH release test on MC3T3 cells. Figure 7A showed the relative cell viability tested by CCK-8 after 24 h of incubation with Alen and different nanoparticles in a series of concentration. The results showed that the relative cell viability was higher than 91% for Alen at 2-50 μg mL^{-1}, implying good biocompatibility of the drug without significant cytotoxicity to those cells. The values corresponding to cells incubated with nanoparticles are ≥100% in most cases, and Alen-loaded nanoparticles ($NP1_{Alen}$, $NP2_{Alen}$ and $NP3_{Alen}$) showed relatively lower cell viability than that of empty nanoparticles ($NP1_{Emp}$, $NP2_{Emp}$ and $NP3_{Emp}$) due to the Alen loading. The viability % increase over 100% even at high nanoparticle concentration (1000 μg mL^{-1}) may be

attributed to the increased surface area available for cell growth resulted by the physical presence of particles.[32] According to previous report, providing a biocompatible environment near small clusters of cells could increase cell aggregation and proliferation rate in that area. [33] Figure 7B showed the LDH release induced by the nanoparticles. LDH, a kind of enzyme catalyzing the conversion of pyruvate to lactate and vice versa, is generally used as an indicator to evaluate cellular and tissue damage, which is released from cells into plasma when cells are damaged or destroyed.[34] The results showed that all the nanoparticles induced LDH release less than 30% at all the tested concentrations (10-300 μg mL^{-1}), indicating that the nanoparticles do not present apparent cytotoxicity, which is in good accordance with the result of CCK-8 test.

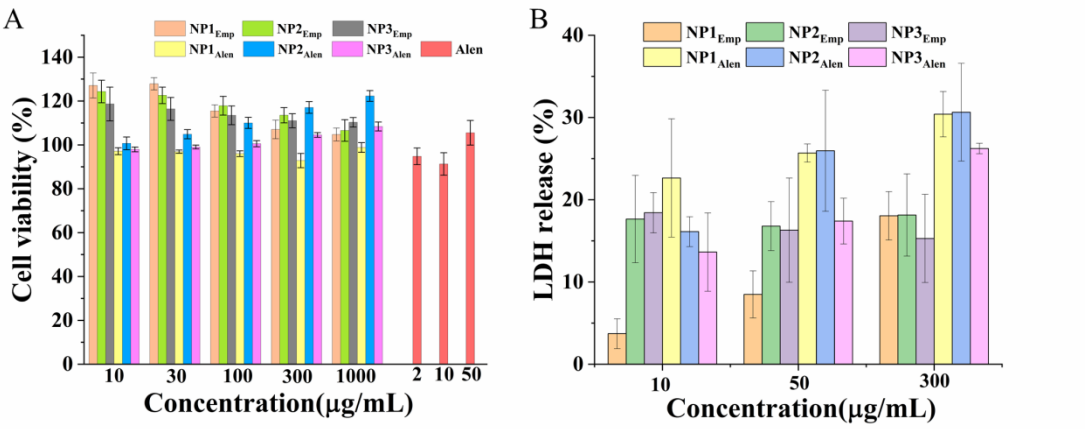

Figure 7. Cytotoxicity of the nanoparticles on MC3T3 cells after incubation at 37 °C for 24 h detected by CCK-8 assay (A) and LDH release test (B).

3.6 Blood biocompatibility

The blood biocompatibility of nanoparticles was investigated by hemolysis test on red blood cells. Hemolysis refers to the rupture phenomenon of RBC, resulting hemoglobin release from RBC into the surrounding medium. It is generally used to

evaluate the blood biocompatibility of biomaterials. The hemolysis rate indicates the extent of RBC broken by the contact between materials and blood, and it is regarded as safe when it is less than 5%.[35] As shown, no significant hemolysis (<5%) was observed when the red blood cells were exposed to a series concentration of different nanoparticles (10-300 μg mL^{-1}) (Figure 8,). The results indicated that the nanoparticles did not disturb RBCs membranes and cause hemolysis to the blood system, which are acceptable for Alen delivery in biomedical applications.

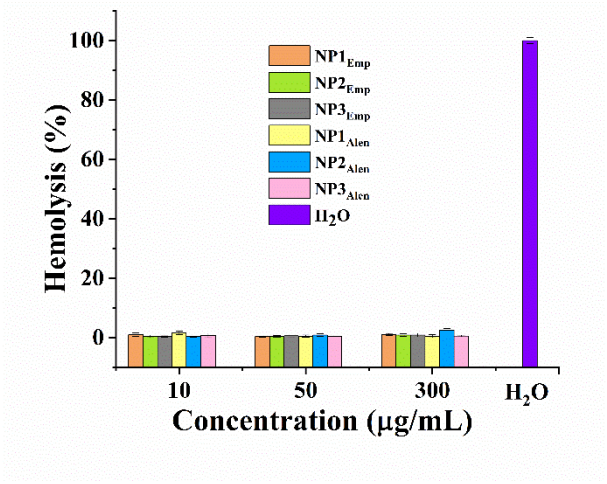

Figure 8. Hemolysis of RBCs (4% v/v) incubated with various concentrations of different nanoparticles.

3.7 Affinity of nanoparticles to HAp disks

For bone-targeted delivery, high affinity to bone tissue is the primary requirement. Thus, HAp disks prepared from HAp nanopowders by compression moulding were used as model bone to evaluate the affinity of nanoparticles to HAp. Figure 9A showed the images of fluorescent intensity for HAp disks after incubation with nanoparticles with or without Alen-decoration for 0.5, 2 and 4 h. As shown, the fluorescent intensity of HAp disks increased with incubation time, and HAp disks incubated with $NP4_{RB}$

(Alen-decorated nanoparticles) exhibited stronger fluorescent intensity compared to that incubated with $NP5_{RB}$ (non-Alen-decorated nanoparticles). Quantified analysis of the fluorescence intensity showed that the amount of $NP4_{RB}$ binding to HAp disks was apparently higher than that of $NP5_{RB}$ (Figure 9B) due to the specific binding of Alen and Ca^{2+} in HAp. In addition, the binding ratio of nanoparticles also increased with incubation time. Figure 9C showed that the ratio of absorbed $NP4_{RB}$ was 12.1, 25.6 and 31.4% at 0.5, 2 and 4 h, respectively, which was significantly higher than that of $NP5_{RB}$, only a small ratio (7.4, 19.1 and 24.3% at 0.5, 2 and 4 h, respectively) of $NP5_{RB}$ were absorbed into the HAp disks. The result of the high affinity to HAp disks of Alen-decorated nanoparticles was attributed to the special binding between Alen and bone minerals, suggesting the feasibility and potential promise of this nanoparticle system in bone-targeted delivery for osteoporosis therapy.

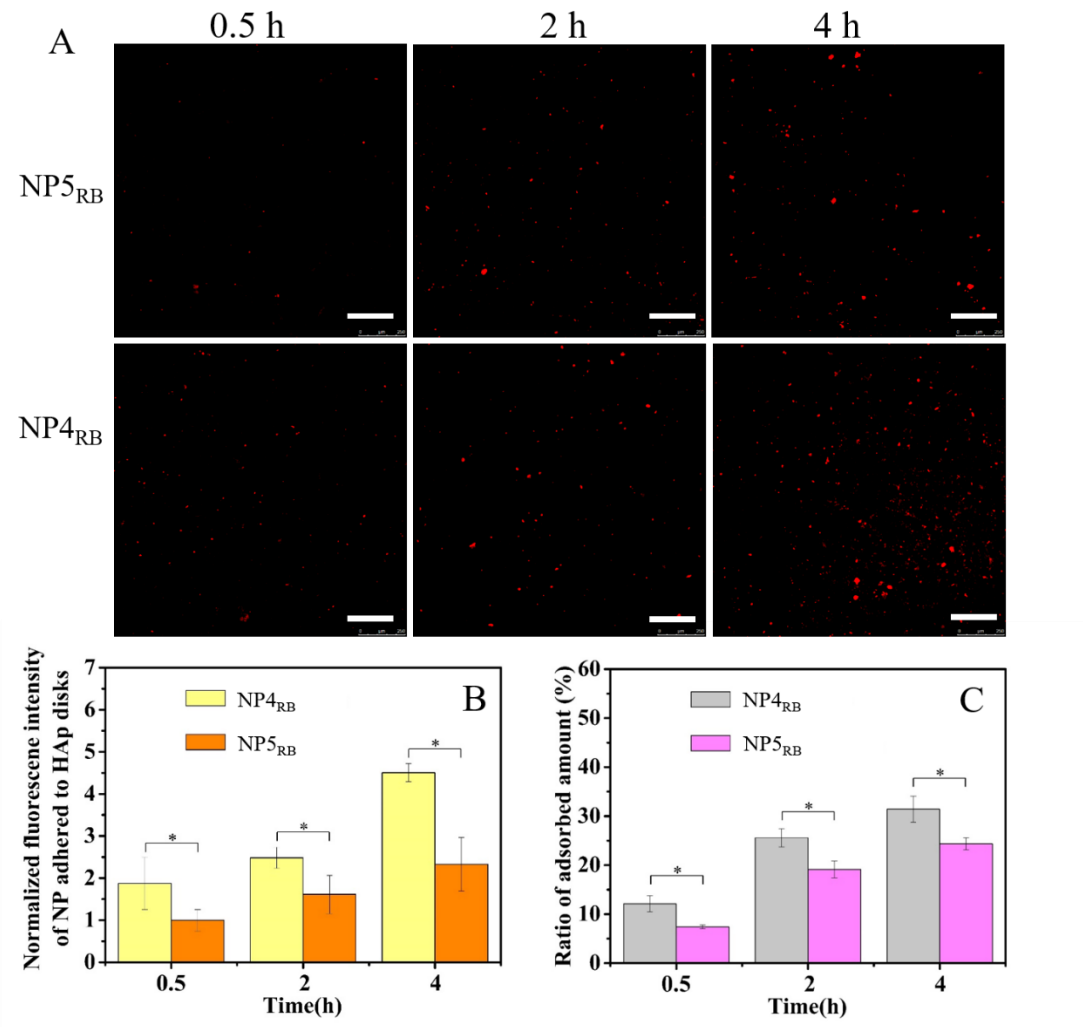

Figure 9. Fluorescence intensity images of HAp disks incubated with $NP4_{RB}$ (nanoparticles with Alen-decoration) and $NP5_{RB}$ (nanoparticles without Alen decoration) observed using CLSM (A). Quantification analysis of nanoparticles (NP) adhered to HAp disks using Image J software. * $p<0.05$. (B). Ratio of adsorbed amount of $NP4_{RB}$ and $NP5_{RB}$ into the HAp disks. * $p<0.01$. (C). The data are presented as mean ±SD. (n=3). Scale bar 250 μm.

4. CONCLUSIONS

Alen-decorated polymeric nanoparticles were fabricated for Alen loading and bone-targeted delivery. PLGA-CS-CD/ALG-Alen nanoparticles with different polymer ratio were synthesized. The nanoparticles were negatively charged with an average size

between ~300-500 nm as determined by DLS. Sustained release of Alen from the nanoparticles was observed, and the drug release behavior could be tuned by changing the polymer ratio. CCK assay and LDH release test on MC3T3 cells showed that the nanoparticles had good cytocompatibility. Hemolysis test showed that the nanoparticles had good blood biocompatibility with low hemolysis ratios (<5%) Moreover, bone affinity test showed that the PLGA-CS-CD/ALG-Alen nanoparticles exhibited a significant higher binding ratio to HAp disks compared with that of nanoparticles without Alen modification. Thus, the PLGA-CS-CD/ALG-Alen nanoparticles are expected to become promising bone-targeted carriers for the treatment of osteoporosis.

Corresponding Authors

*Lingling Zhao (Email: zhaolingling@nbu.edu.cn), *Hui Tan

(Email:huitan@email.szu.edu.cn)

Author Contributions

Lingling Zhao and Hui Tan designed the project and research process. Lingling Zhao and Chunlan Jing completed the draft of the manuscript. Chunlan Jing and Bowen Li carried out the preparation and characterization of nanoparticles. Hongze Liang, Chang Zhang and Shenmao Chen performed data compilation and analysis, Haining Na and Chaozong Liu reviewed and revised the draft. All participants have confirmed the final manuscript without objection.

Notes

The authors declare no competing financial interest.

ACKNOWLEDGMENT

Thanks for the funding by the Basic scientific research operating expenses of provincial universities (SJLY2021002), Science and Technology Innovation Commission of Shenzhen (ZDSYS20200811142600003), Natural Science Foundation of Guangdong Province (2021A1515010720), the K. C. Wong Magna Fund in Ningbo University, and Key Laboratory of Advanced Mass Spectrometry and Molecular Analysis of Zhejiang Province.

REFERENCES

(1) Ossipov, D. A. Bisphosphonate-Modified Biomaterials for Drug Delivery and Bone Tissue Engineering. *Expert Opin. Drug Deliv.* **2015,** *12* (9), 1443-1458.

(2) Delmas, P. D. Treatment of Postmenopausal Osteoporosis. *Lancet.* **2002,** *359*, 2018-26.

(3) Miladi, K.; Sfar, S.; Fessi, H.; Elaissari, A. Encapsulation of Alendronate Sodium by Nanoprecipitation and Double Emulsion: From Preparation to in Vitro Studies. *Ind. Crop. Prod*. **2015,** *72*, 24-33.

(4) Miladi, K.; Sfar, S.; Fessi, H.; Elaissari, A. Drug carriers in osteoporosis：preparation, drug encapsulation and applications. *Int. J. Pharm.* **2013,** *445*, 181-195.

(5) Cohen-Sela, E.; Rosenzweig, O.; Gao, J. C.; Epstein, H.; Gati, I.; Reich, R.; Danenberg, H. D.; Golomb, G. Alendronate-Loaded Nanoparticles Deplete Monocytes and Attenuate Restenosis. *J. Control. Release*. **2006,** *113* (1), 23-30.

(6) Miladi, K.; Sfar, S.; Fessi, H.; Elaissari, A. Enhancement of Alendronate Encapsulation in Chitosan Nanoparticles. *J. Drug Deliv. Sci. Technol.* **2015,** *30,* 391-396.

(7) Shi, C.; Wu, T.; He, Y.; Zhang, Y.; Fu, D. Recent Advances in Bone-Targeted Therapy. *Pharmacol. Ther.* **2020,** *207*, 107473.

(8) Ryu, T. K.; Kang, R. H.; Jeong, K. Y.; Jun, D. R.; Koh, J. M.; Kim, D.; Bae, S. K.; Choi, S. W. Bone-Targeted Delivery of Nanodiamond-Based Drug Carriers Conjugated with Alendronate for Potential Osteoporosis Treatment. *J. Control. Release.* **2016,** *232*, 152-60.

(9) Wang,Y. Y.; Yao, J.; Cai, L. Z.; Liu, T.; Wang, X. G.; Zhang, Y.; Zhou, Z. Y.; Li, T. W.; Liu, M. Y.; Lai, R. F.; Liu, X. N. Bone-Targeted Extracellular Vesicles from Mesenchymal Stem Cells for Osteoporosis Therapy. *Int. J. Nanomed.* **2020 ,** *15*, 7967-7977.

(10) Li, L.; Yu, M.; Li, Y.; Li, Q.; Yang, H.; Zheng, M.; Han, Y.; Lu, D.; Lu, S.; Gui, L. Synergistic Anti-Inflammatory and Osteogenic n-HA/Resveratrol/Chitosan Composite Microspheres for Osteoporotic Bone Regeneration. *Bioact. Mater.* **2021,** *6* (5), 1255-1266.

(11) Vinay, R.; KusumDevi, V. Potential of Targeted Drug Delivery System for the Treatment of Bone Metastasis. *Drug Deliv.* **2016,** *23*(1), 21-29.

(12) Levengood, S. K. L.; Zhang, M. Q. Chitosan-based Scaffolds for Bone Tissue Engineering. *J. Mat. Chem. B.* **2014,** *2*(21), 3161-3184.

(13) Yuan, Z.; Wei, P.; Huang, Y.; Zhang, W.; Chen, F.; Zhang, X.; Mao, J.; Chen, D.; Cai, Q.; Yang, X. Injectable PLGA Microspheres with Tunable Magnesium Ion Release for Promoting Bone Regeneration. *Acta Biomater.* **2019,** *85*, 294-309.

(14) Liu, L.; Huang, B.; Liu, X.; Yuan, W.; Zheng, Y.; Li, Z.; Yeung, K. W. K.; Zhu, S.; Liang, Y.; Cui, Z.; Wu, S. Photo-Controlled Degradation of PLGA/Ti_3C_2 Hybrid Coating on Mg-Sr Alloy using Near Infrared Light. *Bioact. Mater.* **2021,** *6* (2), 568-578.

(15) Thakur, C. K.; Thotakura, N.; Kumar, R.; Kumar, P.; Singh, B.; Chitkara, D.; Raza, K. Chitosan-Modified PLGA Polymeric Nanocarriers with Better Delivery Potential for Tamoxifen. *Int. J. Biol. Macromol.* **2016,** *93*, 381-389.

(16) Hu, X.; Chen, S.; Yin, H.; Wang, Q.; Duan, Y.; Jiang, L.; Zhao, L. Chitooligosaccharides-Modified PLGA Nanoparticles Enhance the Antitumor Efficacy of AZD9291 (Osimertinib) by Promoting Apoptosis. *Int. J. Biol. Macromol.* **2020,** *162*, 262-272.

(17) Monteil, M.; Lecouvey, M.; Landy, D.; Ruellan, S.; Mallard, I. Cyclodextrins: A Promising Drug Delivery Vehicle for Bisphosphonate. *Carbohydr. Polym.* **2017,** *156*, 285-293.

(18) Yin, Y.; Yang, M.; Xi, J.; Cai, W.; Yi, Y.; He, G.; Dai, Y.; Zhou, T.; Jiang, M. A Sodium Alginate-Based Nano-Pesticide Delivery System for Enhanced in Vitro Photostability and Insecticidal Efficacy of Phloxine B. *Carbohydr. Polym.* **2020,** 247, 116677.

(19) Ravichandran, V.; Jayakrishnan, A. Synthesis and Evaluation of Anti-Fungal Activities of Sodium Alginate-Amphotericin B Conjugates. *Int. J. Biol. Macromol.* **2018,** *108*, 1101-1109.

(20) Campos, E. V. R.; de Oliveira, J. L.; Fraceto, L. F.; Singh, B. Polysaccharides as Safer Release Systems for Agrochemicals. *Agron. Sustain. Dev.* **2015,** *35* (1), 47-66.

(21) Farshi Azhar, F.; Olad, A. A Study on Sustained Release Formulations for Oral Delivery of 5-Fluorouracil Based on Alginate-Chitosan/Montmorillonite Nanocomposite Systems. *Appl. Clay Sci.* **2014,** *101*, 288-296.

(22) Yang, Y.; Liu, Y.; Chen, S.; Cheong, K. L.; Teng, B. Carboxymethyl Beta-Cyclodextrin Grafted Carboxymethyl Chitosan Hydrogel-Based Microparticles for Oral Insulin Delivery. *Carbohydr. Polym.* **2020,** *246*, 116617.

(23) Wu, Z. M.; Zhang, S. M.; Zhang, X. G.; Shu, S. J.; Chu, T. C.; Yu, D. M. Phenylboronic Acid Grafted Chitosan as a Glucose-Sensitive Vehicle for Controlled Insulin Release. *J. Pharm. Sci.* **2011,** *100* (6), 2278-2286.

(24) Zhao, L. L.; Zhang, Y. J.; Shao, J.; Liang, H. Z.; Na, H. N.; Zhu, J. Folate-Conjugated Dually Responsive Micelles for Targeted Anticancer Drug Delivery. *RSC Adv.* **2016,** *6* (42), 35658-35667.

(25) Karthikeyan, P.; Meenakshi, S. In-Situ Fabrication of Cerium Incorporated Chitosan-β-Cyclodextrin Microspheres as an Effective Adsorbent for Toxic Anions Removal. *Environ Nanotechnology. Monit. Manage.* **2019,** 12, 100272.

(26) Balbino, T. A. C.; Bellato, C. R.; da Silva, A. D.; Marques Neto, J. d. O.; Guimarães, L. d. M. Magnetic Cross-Linked Chitosan Modified with Ethylenediamine and β-Cyclodextrin for Removal of Phenolic Compounds. *Colloid Surf. A-Physicochem. Eng. Asp.* **2020,** *602,* 125119.

(27) Arafa, M. G.; Mousa, H. A.; Afifi, N. N. Preparation of PLGA-Chitosan Based Nanocarriers for Enhancing Antibacterial Effect of Ciprofloxacin in Root Canal Infection. *Drug Deliv.* **2020,** *27*(1), 26-39.

(28) Li, J.; Hu, W. Q.; Zhang, Y. J.; Tan, H.; Yan, X. J.; Zhao, L. L.; Liang, H. Z. pH and Glucose Dually Responsive Injectable Hydrogel Prepared by In Situ Crosslinking of Phenylboronic Modified Chitosan And Oxidized Dextran. *J. Polym. Sci. Pol. Chem.* **2015,** *53* (10), 1235-1244.

(29) Song, M. M.; Li, L. P.; Zhang, Y.; Chen, K. M.; Wang, H.; Gong, R. M. Carboxymethyl-β-cyclodextrin Grafted Chitosan Nanoparticles as Oral Delivery Carrier of Protein Drugs. *React. Funct. Polym.* **2017,** *117*, 10-15.

(30) Darvishi, M. M.; Moazeni, M.; Alizadeh, M.; Abedi, M.; Tamaddon, A. M. Evaluation of the Efficacy of Albendazole Sulfoxide (ABZ-SO)-Loaded Chitosan-PLGA Nanoparticles in the Treatment of Cystic Echinococcosis in Laboratory Mice. *Parasitol. Res.* **2020,** *119* (12), 4233-4241.

(31) Hwang, S. J.; Lee, J. S.; Ryu, T. K.; Kang, R. H.; Jeong, K. Y.; Jun, D. R.; Koh, J. M.; Kim, S.E.; Choi, S.W. Alendronate-Modified Hydroxyapatite Nanoparticles for Bone-Specific Dual Delivery of Drug And Bone Mineral. *Macromol. Res.* **2016,** *24* (7), 623-628.

(32) Matrali, S. S. H.; Ghag, A. K. Feedback-Controlled Release of Alendronate from Composite Microparticles. *J. Funct Biomater.* **2020,** *11* (3), 46.

(33) Fu, B.; Sun, X.; Qian, W.; Shen, Y.; Chen, R.; Hannig, M. Evidence of Chemical Bonding to Hydroxyapatite by Phosphoric Acid Esters. *Biomaterials* **2005,** *26* (25), 5104-5110.

(34) Su, F.; Wang, Y.; Liu, X.; Shen, X.; Zhang, X.; Xing, Q.; Wang, L.; Chen, Y. Biocompatibility and in vivo Degradation of Chitosan Based Hydrogels as Potential Drug Carrier. *J. Biomater Sci Polym Ed.* **2018,** *29* (13), 1515-1528.

(35) Song, S. J.; Lee, S.; Ryu, K. S.; Choi, J. S. Amphiphilic Peptide Nanorods Based on Oligo-Phenylalanine as a Biocompatible Drug Carrier. *Bioconjugate Chem.* **2017,** *28* (9), 2266-2276.

Graphic for manuscript